Simulations of the Modular Axisymmetric Scramjet Test Rig Under Reacting Flow Conditions

Jacob Lampenfield
Analytical Mechanics Associates Inc
Tom Drozda, Matthew O'Connell
Hypersonic Air-Breathing Propulsion Branch (HAPB), NASA Langley Research Center
Tim Ombrello
AFRL, WPAFB

JANNAF, December 2023

Introduction

Motivation:

Supersonic combustion ramjet (scramjet) powerhead design, leading to efficient fuel-air mixing, flame- holding, and combustion remains one of the key challenges in scramjet flowpath design

- Flameholding devices are typically employed to support robust and stable combustion
  - Intrusive methods, aerodynamic wakes of strut injectors
  - Non-intrusive method, cavity flameholders
- The Modular Axisymmetric Scramjet Test Rig (MASTeR) is a new 1X-scale axisymmetric combustor expected to be tested in Research Cell 19 (RC19) at AFRL over the next couple of years

Goals:

1. Demonstrate the application of an automated unstructured grid adaptation tool in VULCAN-CFD for reacting Reynolds-averaged simulations (RAS)
2. Explore the experimental space of MASTeR to provide a high-level understanding about operating performance

MASTeR Geometry

- Axisymmetric modular test article
- Mach 2 or 3 facility nozzle
- Variable length (L) and depth (D) cavity flame holder, depths of 0.25, 0.75, and 1.25 inches, and L/D of 4, 6, and 8
- 32 primary injectors and 16 secondary injectors with a diameter of 0.05 inches

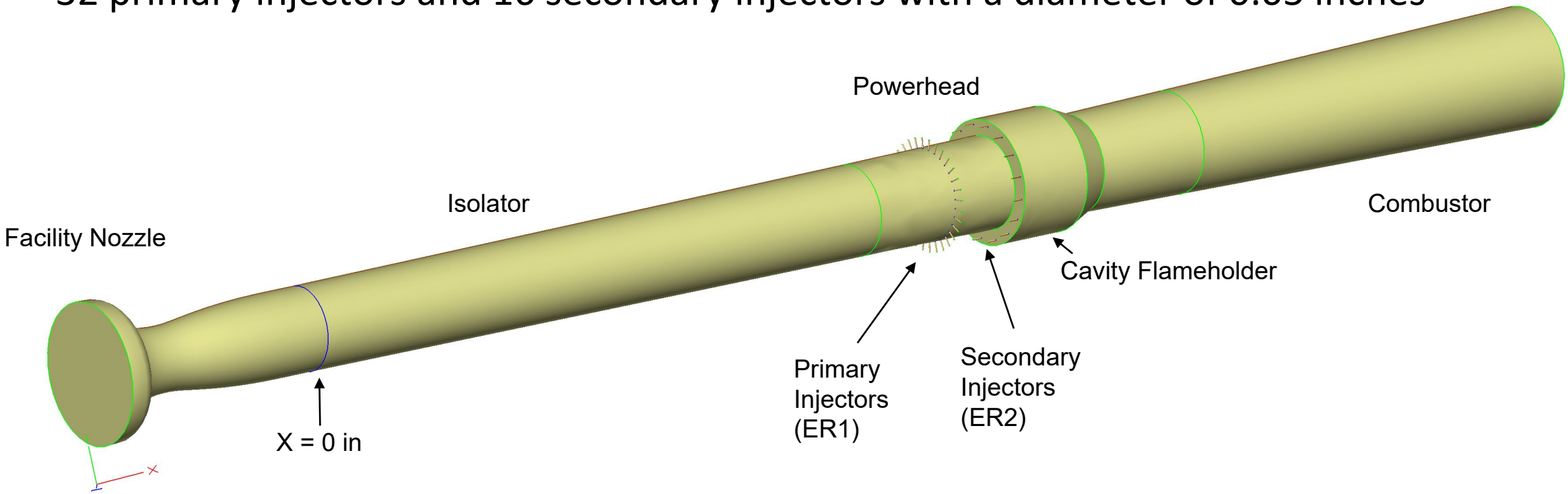

Flow Conditions

Property	Air	Fuel (Ethylene)
Mach	2.0	Varies
P_0 (psi)	50	Varies
T_0 (F)	600	80
Mole Fraction	79% N 21% O2	100%

Independent Variables	
ER1 (Primary Injector)	0.04-0.4
ER2 (Secondary Injector)	0.01-0.2
L/D	4, 6, 8

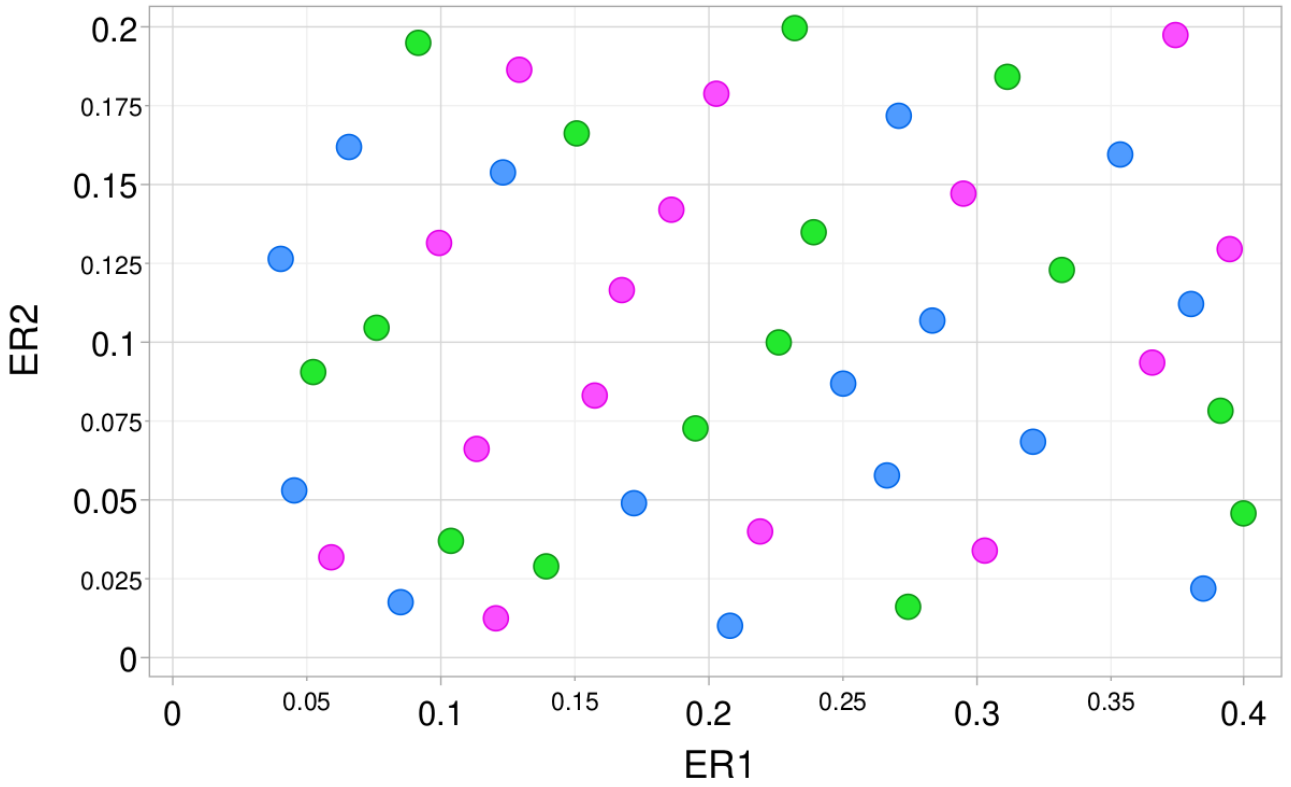

- Latin hypercube sampling (LHS) was used to generate a list of cases to simulate
- A total of 45 cases were simulated (15 for each L/D) resulting in 450 auto-generated grids
- The colors green, blue, and magenta denote the L/D values of 4, 6, and 8, respectively

Numerical Simulation Details

- VULCAN-CFD used as flow solver
- Unstructured 3D Reynolds-averaged simulations (RAS)
- Advective terms computed using a MUSCL scheme with the Low-Dissipation Flux-Split Scheme (LDFSS)
- Governing equations integrated using the Symmetric Gauss-Seidel (SGS) method
- Menter Baseline blended k-ω/k−ε turbulence model
- Thermodynamic properties of mixture components computed using McBride curve fits
- Reynolds heat and species mass fluxes modeled using a gradient diffusion model, turbulent $Pr_t = 0.9$, turbulent $Sc_t = 0.5$
- Wilcox wall matching functions used where appropriate
- Chemical reactions modeled using 6-species, 3-reaction reduced chemical kinetics model

Adaptation Methodology Flowchart

- Computational geometry is built using Engineering Sketch Pad (ESP)
- After the geometry is built, the initial mesh is created using Tetgen and passed to *refine*
- CFD simulations commence, and new grids are adapted using *refine* based on error estimates of a specified flow field parameter (e.g., Mach number) obtained from CFD simulations

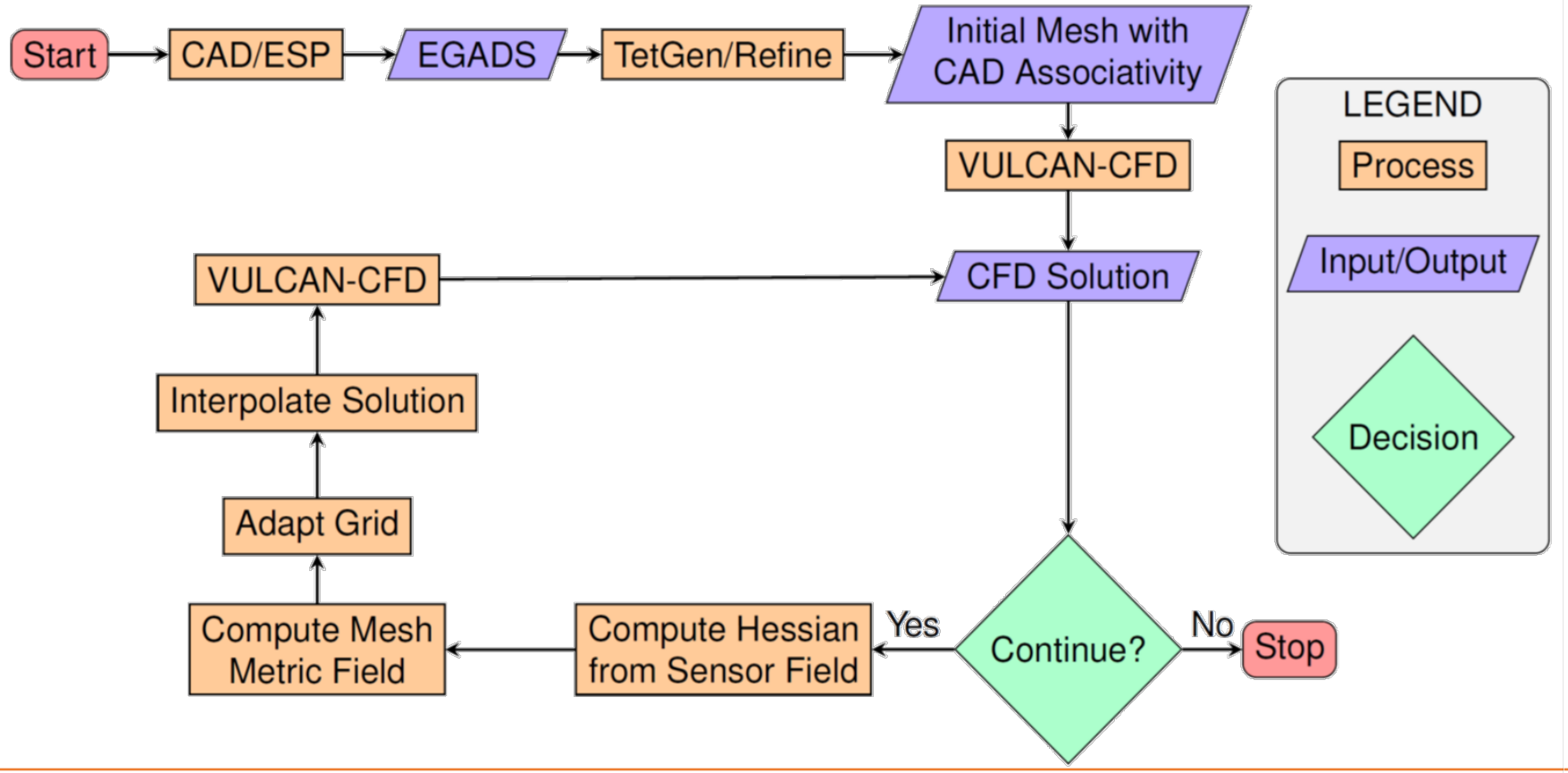

Adaptation Methodology

Aggressive strategy adapts grids more rapidly

- Adaptation uses 1 “smoothing” stage, called a stride, after which grid count is doubled
- Simulations for adaptations 1-3 utilize only 1st-order numerics
- Simulations for adaptations 1-5 utilize an ignition sub-domain spanning the cavity flameholder volume
- Simulations for adaptation 6-10 utilize 2nd-order numerics and ignition sub-domain was turned off

Adaptation	Grid Cells
1	121,135
4	240,652
6	485,260
8	936,533
10	1,892,995

Grid 1

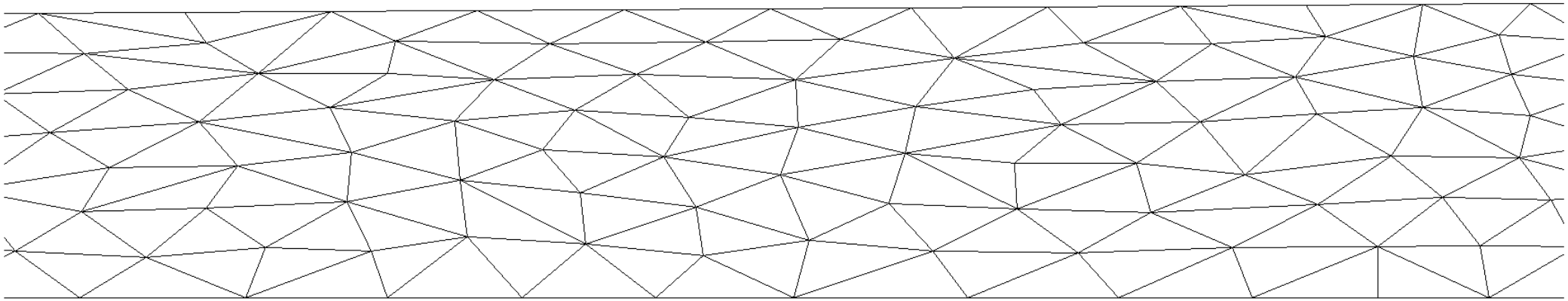

Animation of the grid refinement around the shock train formed upstream of the powerhead due to backpressure from combustion

Results: Adaptation Solution Progression

- First grid is very coarse and does not resolve the boundary layers
  - Simulation introduces near-wall gradients which prompts *refine* to initiate grid clustering
- By grid four, boundary layer and stronger shocks are being refined
- By grid six, downstream interacting shocks are identified
- Flow features are refined and user-determined grid convergence is reached by grid 10

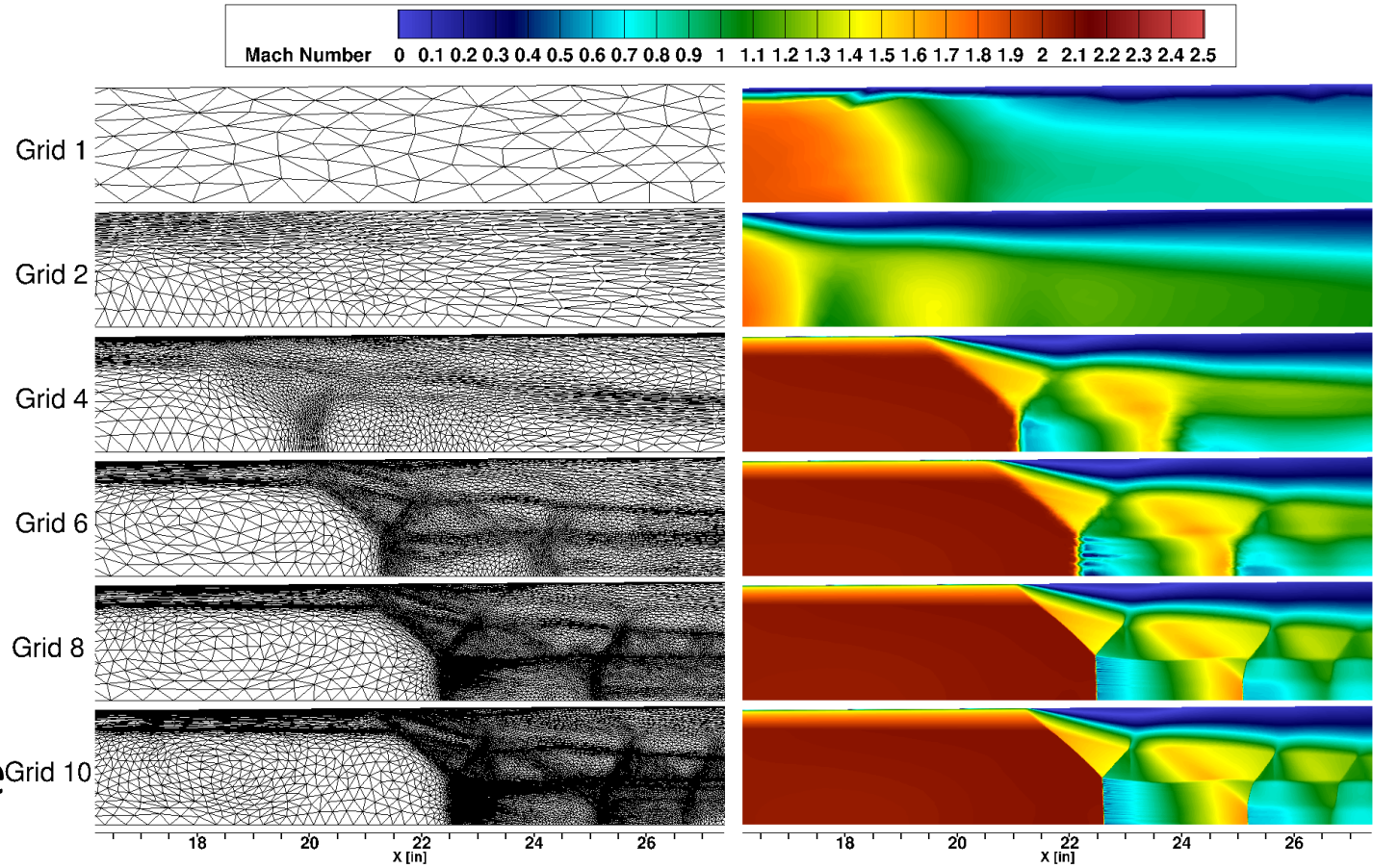

Metrics of Interest and Convergence

- Mixing efficiency and combustion efficiency are used to assess rate of convergence

$$\eta_m = \frac{\int \alpha_R \rho u dA}{\int \alpha \rho u dA}$$

$$\eta_c = 1 - \frac{\dot{m}_f}{\dot{m}_{f,tot}}$$

- Unstructured grid convergence assessed by examining change in mixing efficiency and combustion efficiency with grid adaptation. User subjectively determines the change between solutions is "small enough"

Metrics of Interest

- Equivalence ratio (ER) is evaluated at several locations in the cavity
- These locations help characterize the extent of variation of flow properties in the cavity

$$ER = \frac{F/O}{(F/O)_{st}} = \frac{1 - f_{st}}{f_{st}} \frac{f}{1 - f}$$

Mixture fraction

$$f = Y_{C_2H_4} + \frac{W_{C_2H_4}}{6}\left(\frac{2Y_{CO_2}}{W_{CO_2}} + \frac{Y_{H_2O}}{W_{H_2O}} + \frac{2Y_{CO}}{W_{CO}} + \frac{Y_{H_2}}{W_{H_2}}\right)$$

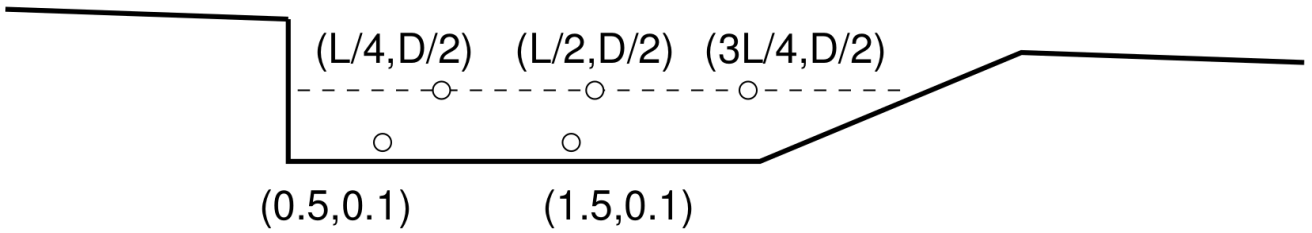

Schematic of the cavity flameholder with circles denoting lactations where ER and other quantities are extracted from the simulations

Results: Mixing Efficiency (ER1=0.208, ER2=0.01, L/D=6)

- Only the cavity region is displayed, and both sets of fuel injectors are intended to fuel only the cavity
- Grids 2 and 4 are not shown because the ignition sub-domain was present
- By grid 10 the change in mixing efficiency was deemed to be small enough for this exploratory study

- The fuel from the primary injectors rapidly mixes until the start of the cavity
- The drop in mixing efficiency at the start of the cavity is due to additional fuel added through the secondary cavity injector
- The mixing after the start of the cavity displays a less rapid rate

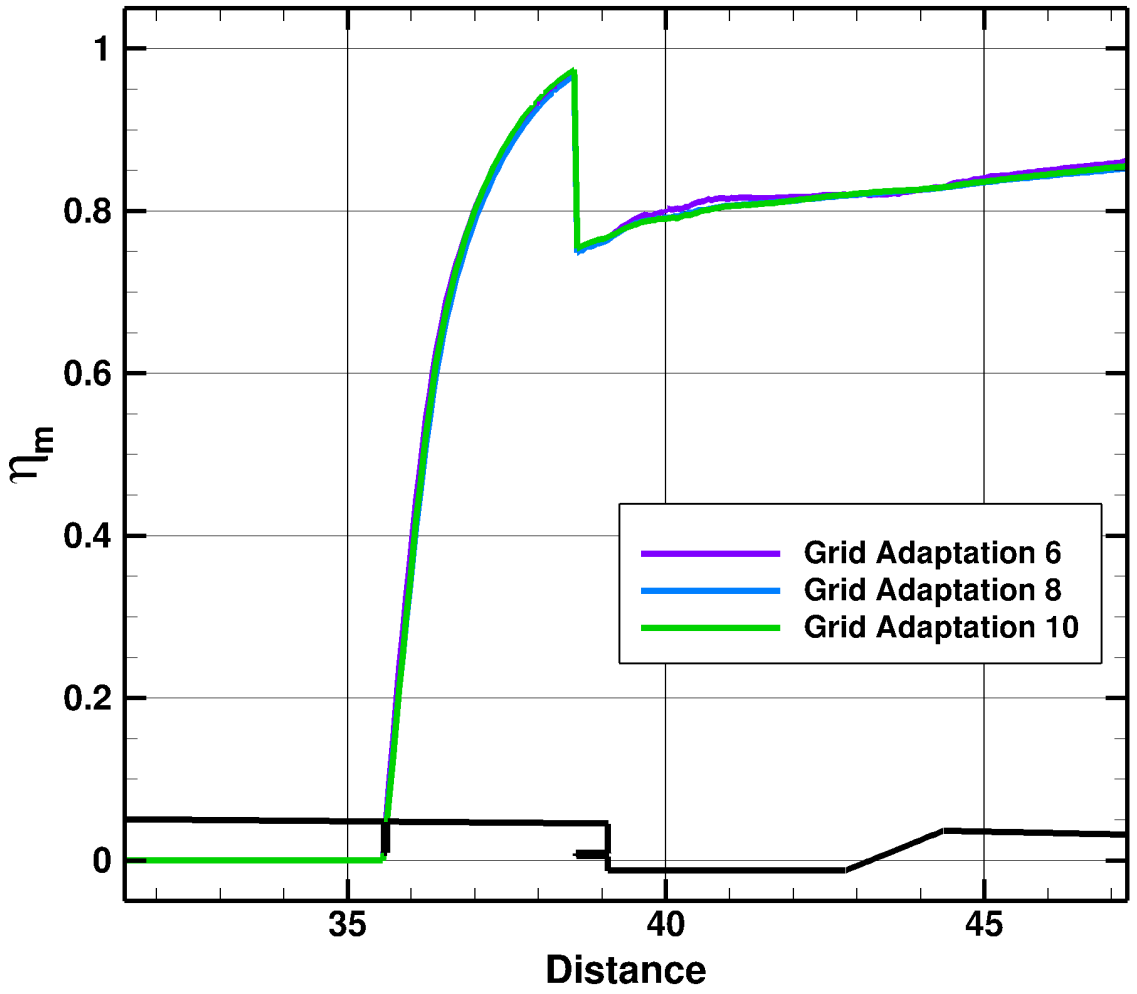

Results: Combustion Efficiency (ER1=0.208, ER2=0.01, L/D=6)

- The change in combustion efficiency with adaptation is more pronounced than that for the mixing efficiency
- However, by grid 10 the change in combustion efficiency was also deemed to be small enough for this exploratory study

- Mixed fuel does not auto ignite upstream of the cavity even though the primary injectors create a wake and counter-rotating vortex pairs which provide some flameholding potential
- Combustion begins to occur once the mixed fuel reaches the cavity
- Combustion continues at a robust rate after the cavity, which indicates that the cavity flameholder is operating as intended

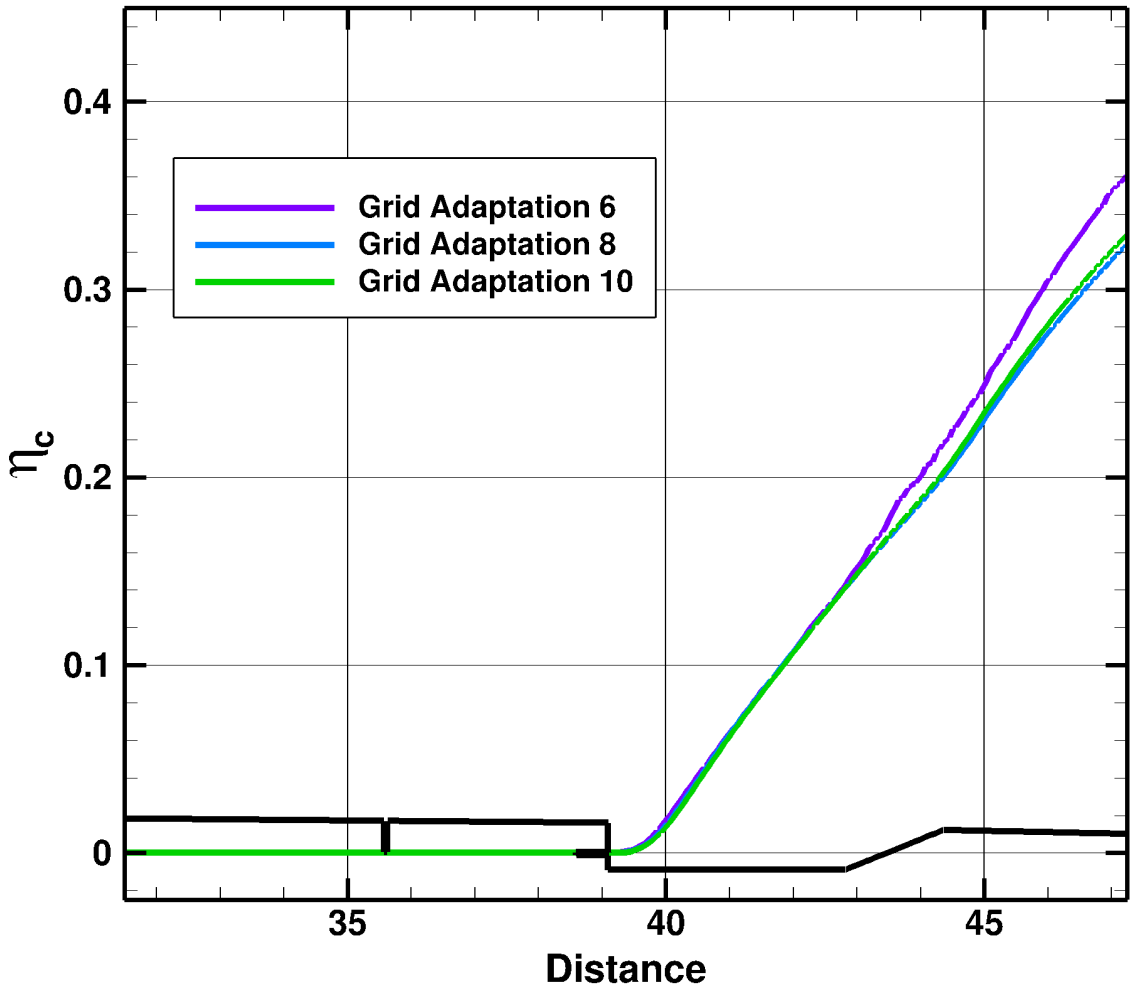

Results from a cavity L/D of 6, ER1 = 0.208 and ER2 = 0.01

Results: Cavity ER Contours (ER1=0.208, ER2=0.01, L/D=6)

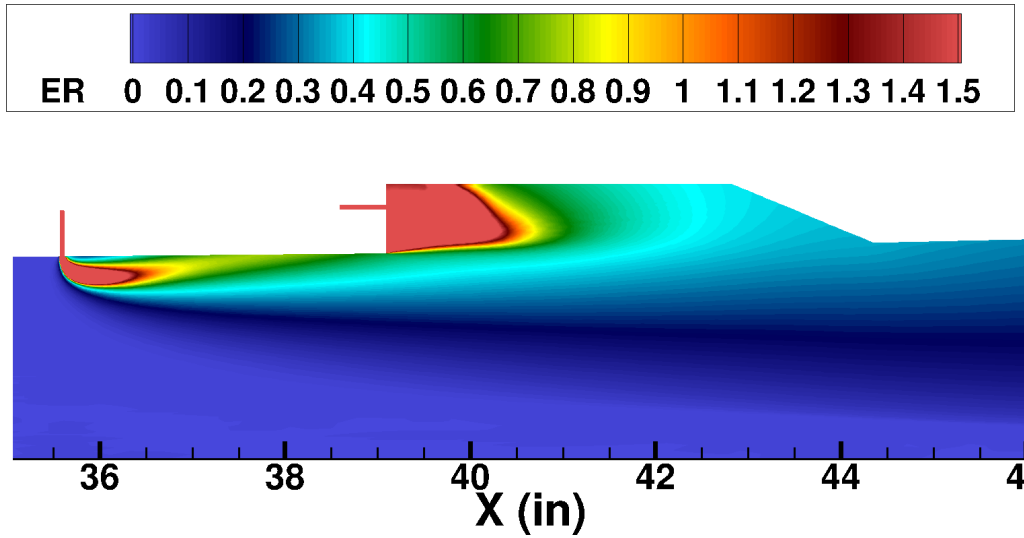

- Slices are through the cavity injector (left) and between cavity injector (right)
- Fuel from upstream injector travels along the wall and is entrained into the cavity with some fuel bypassing the cavity and traveling into the core flow
- Fuel from cavity injector stays closer to the cavity backward face

Results: Cavity Static Temperature Contours (ER1=0.208, ER2=0.01, L/D=6)

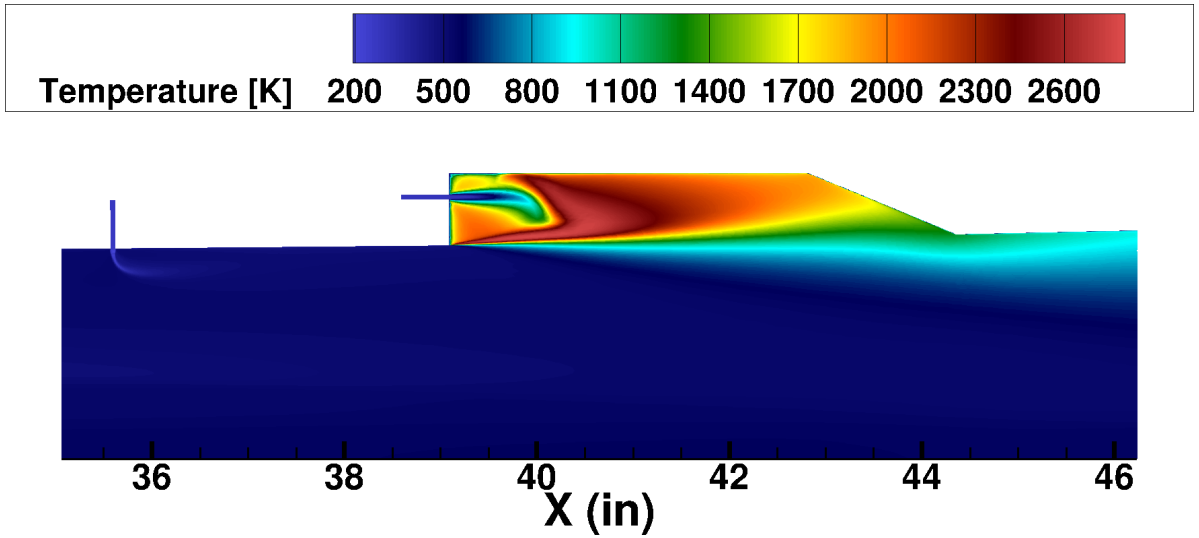

- Slices are through the cavity injector (left) and between cavity injector (right)
- Both symmetry planes indicate high temperatures and robust combustion inside the cavity
- The cold fuel from the secondary cavity injector does not ignite immediately and needs a rise in temperature from the surrounding air to start burning
- Combustion products convect out of the cavity and mix into the remaining fuel to initiate combustion downstream of the cavity

Results: Scatter Plot

- Strong correlation between total ER and leading shock train location (fuel is burning even at high ER1 and ER2)
- Weak correlation between total ER and local cavity ER (approx. the same amount of fuel gets entrained into the cavity independently of the amount of ER1)
- Pronounced correlation between the local cavity ER and the combustion efficiency at the exit of the combustor (cavity is doing its job of flameholding except maybe for the highest values of total ER, ie high ER1 and ER2)
- Correlation between the combustion efficiency and shock train location (shocktrain movement is driven by combustion)

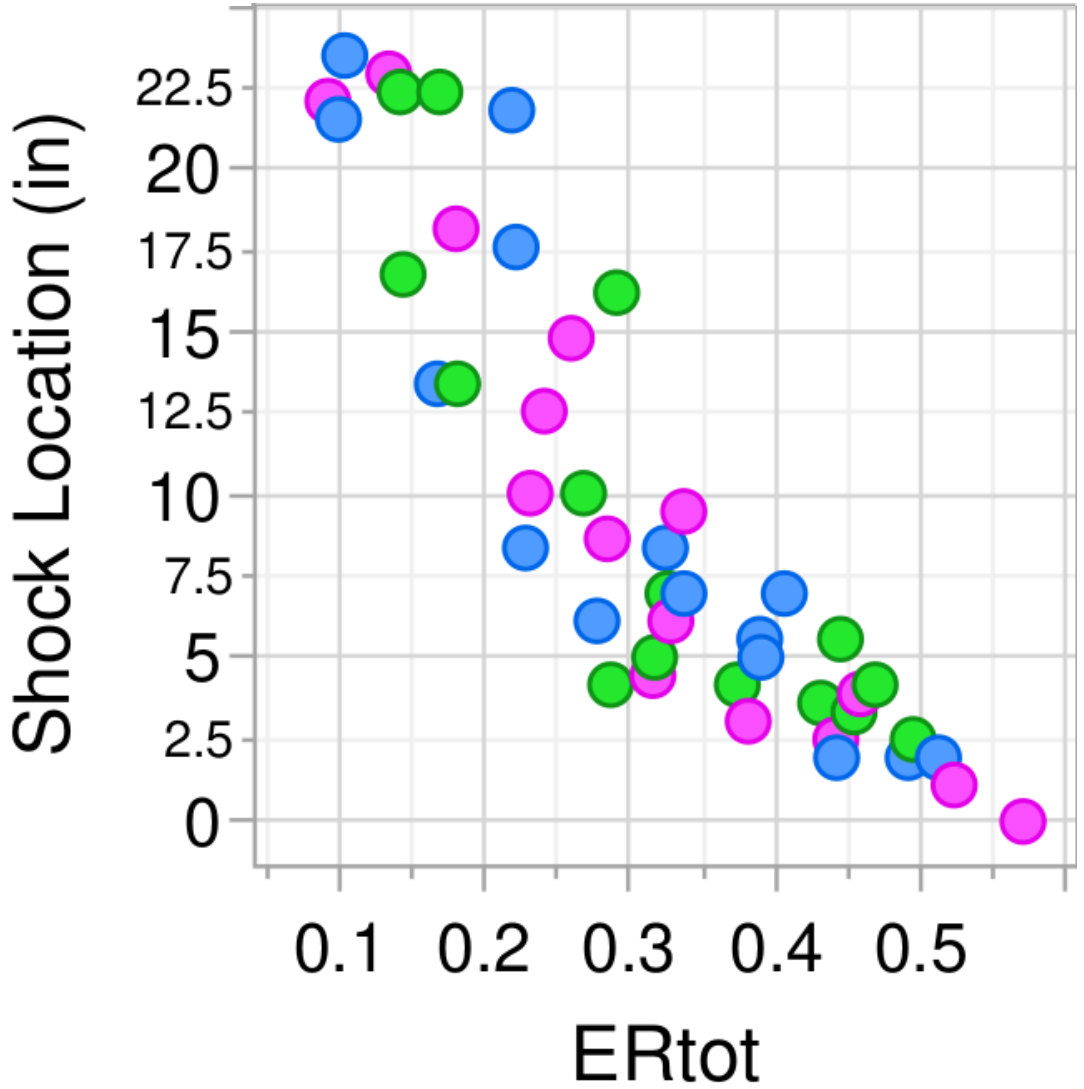

The colors green, blue, and magenta denote the L/D values of 4, 6, and 8, respectively

Results: Scatter Plot All Metrics

- There are at most weak correlations between ER1 and other quantities (indicating that the amount of fuel entering the cavity is approx. independent of ER1)
- The correlation between combustion efficiency at the end of the cavity and ER1 is an indicator that increasing amount of unburnt fuel is bypassing the cavity (expected with increasing ER1)
- The mixing efficiency for many of the lower ER1 values reach 1 by the end of the cavity.
- These cases also correspond to the low ER2 values. But, for higher ER2 values, mixing efficiency decreases.
- No correlation between ER2 and combustion efficiency (fuel is burning well in the cavity but outside has not ignited)
- Strong correlations between ER2 and local cavity ER, static temperature, and water mass fraction.
- Flamelet-like correlations emerges for ER2 and temperature and water mass fraction.

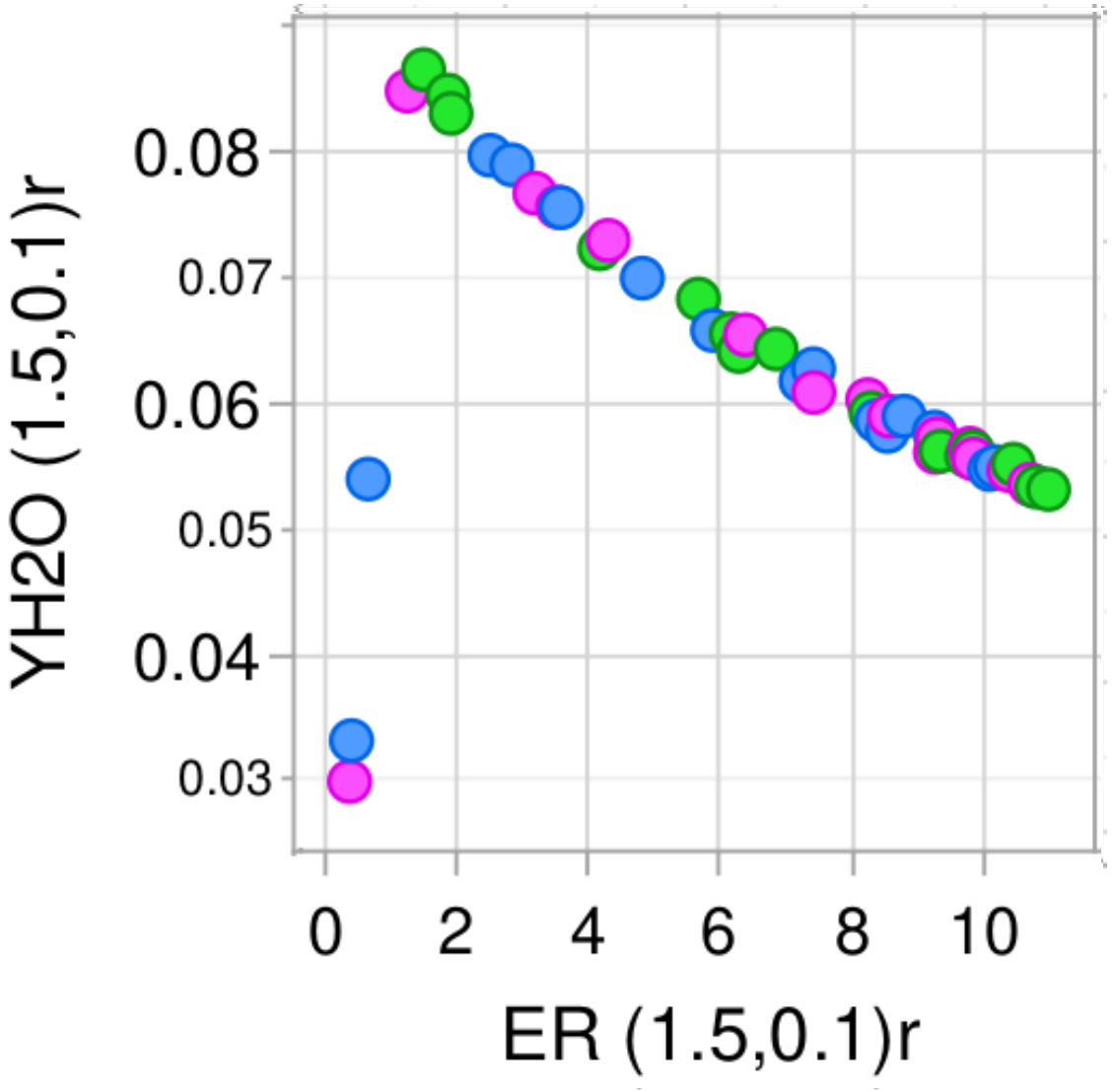

The colors green, blue, and magenta denote the L/D values of 4, 6, and 8, respectively

Summary and Conclusions

- The automated unstructured grid generation and adaptation tool was used to provide knowledge of the operating performance of the MASTeR.
- The correlations between the independent variables ER1 and ER2, and the metrics of interest such as mixing efficiency, combustion efficiency, local ER, and isolator shock train location were determined.
- The cavity operated robustly and somewhat independently of the core flow.
- There was a positive correlation between the local ER measured in the cavity and combustor efficiency at the combustor exit.
- The total injected ER correlated well with the shock train upstream position.
- The local cavity ER was not correlated with the amount of fuel injected upstream of the cavity (ER1) which indicates that about the same amount of fuel is entrained into the cavity independently of ER1

Acknowledgements

This work is supported by the Hypersonic Technology Project (HTP) in the Advanced Air Vehicles Program (AAVP) of the NASA Aeronautics Research Mission Directorate (ARMD). Computational resources are provided by the NASA Langley Research Center and the NASA Advanced Supercomputing (NAS) Division.

Results: Scatter Plot Local ER

- No clear correlations between ER1 and local cavity ER. The fuel from upstream injector that enters the cavity does not significantly change when increasing ER1.
- Correlations between ER2 and all local cavity ER locations.
- All local ER values are correlated with each other. The fuel and air are uniformly mixed in the cavity.
- The L/D=4 cavity (denoted by green markers) appears to produce the most uniform mixtures in the cavity.
- The strength of the correlations increase the farther downstream the local
- ER value is probed, i.e., the clustering of the points about a trendline is well defined. This is due to the fuel mixing more the farther downstream it travels.

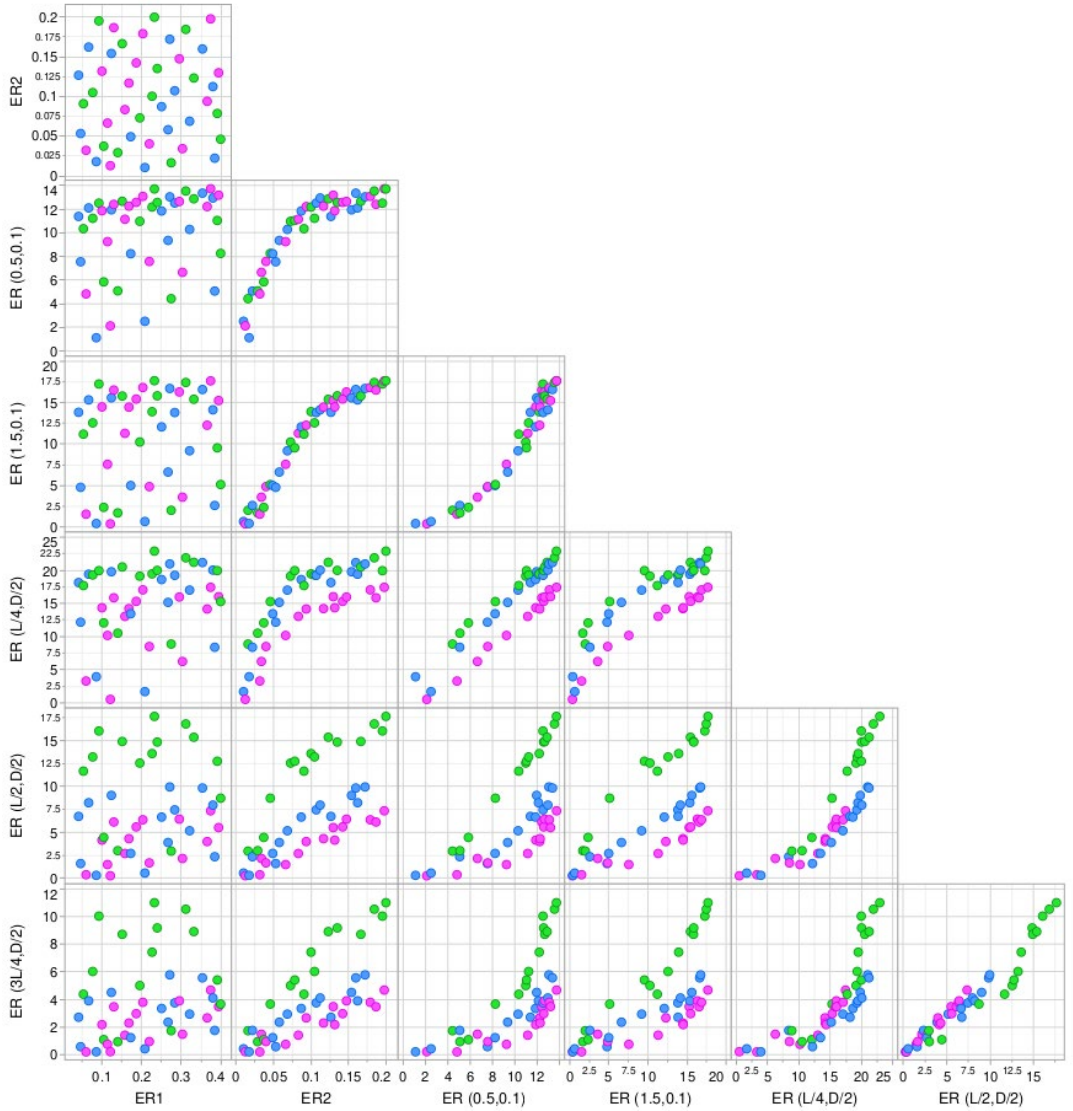

The colors green, blue, and magenta denote the L/D values of 4, 6, and 8, respectively

Results: Scatter Plot Static Temperature

- The static temperatures are somewhat independent of ER1.
- A flamelet-like correlation emerges for ER2, especially for the two near-wall (i.e., 0.1) probe locations.
- For the other probe locations, this flamelet-like correlation between static temperature and ER2 can be observed for the individual values of cavity L/D.
- The static temperatures are also well correlated at various locations. These correlations emerge as vertical clusters that “tilt” toward linear correlation as the data is compared with the downstream probes.

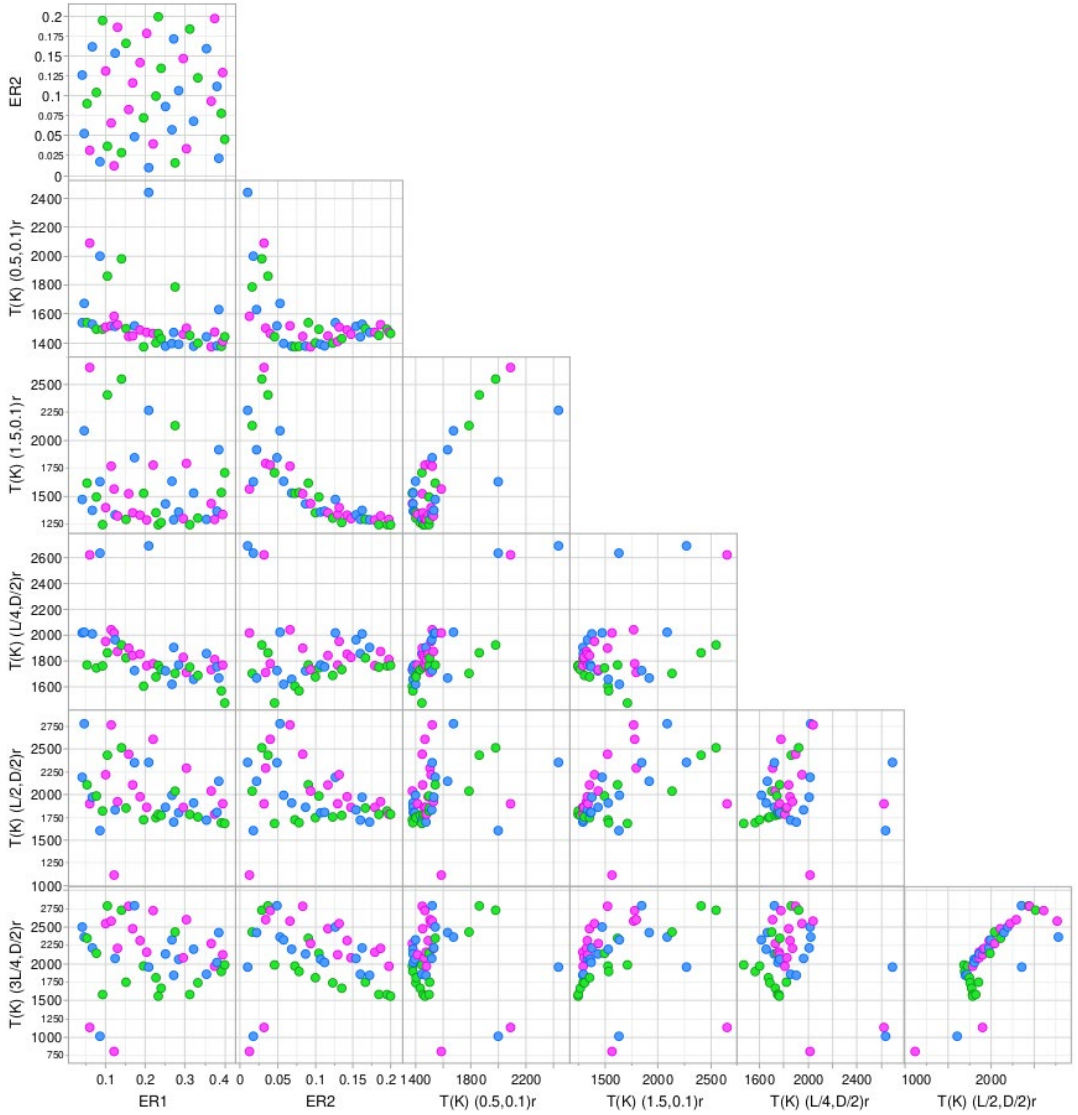

Results: Scatter Plot Water Mass Fraction

- The character of correlations between ER1 and ER2, and water mass fraction is comparable to that found for the temperature.
- For all locations, the mass fraction of water tends to approach similar values regardless of ER1.
- The very lean overall and lean in-cavity cases (larger symbols) are below the group clustering. The local ER in the cavity could be approaching the local extinction limit
- ER2 follows a flamelet-like characteristics, with peak water mass fraction around stoichiometry and decreasing values away from it.
- The water mass fractions are well correlated with each other except for a few outlier cases. These correlations emerge as vertical clusters that turn toward linear correlation as the ER values increase.